Imaging the Two Gaps of the High Temperature Superconductor Pb-$Bi_2Sr_2CuO_{6+x}$

by

Ming Yi

Submitted to the Department of Physics in partial fulfillment of the Requirements for the Degree of

Bachelor of Science in Physics

at the

MASSACHUSETTS INSTITUTE OF TECHNOLOGY

June 2007

Signature of Author_____

Department of Physics
May 11, 2007

Certified by_____

Professor Eric W. Hudson
Thesis Supervisor, Department of Physics

Accepted by_____

Professor David E. Pritchard
Senior Thesis Coordinator, Department of Physics

Imaging the Two Gaps of the High Temperature Superconductor Pb-$Bi_2Sr_2CuO_{6+x}$

by

Ming Yi

Submitted to the Department of Physics
on May 11, 2007, in partial fulfillment of the
requirements for the Degree of
Bachelor of Science in Physics

Abstract

The nature and behavior of electronic states in high temperature superconductors are the center of much debate. The pseudogap state, observed above the superconducting transition temperature T_c, is seen by some as a precursor to the superconducting state. Others view it as a competing phase. Recently, this discussion has focused on the number of energy gaps in the system. Some experiments indicate a single energy gap, implying that the pseudogap is a precursor state. Others indicate two, suggesting that it is a competing or coexisting phase. In this thesis, I report temperature dependent scanning tunneling spectroscopy of Pb-$Bi_2Sr_2CuO_{6+\delta}$. I have developed a novel analytical method that reveals a new, narrow, homogeneous gap that vanishes near T_c, superimposed on the typically observed, inhomogeneous, broad gap, which is only weakly temperature dependent. These results not only support the two gap picture, but also explain previously troubling differences between scanning tunneling microscopy and other experimental measurements.

Thesis Supervisor: Professor Eric W. Hudson

Title: Thesis Supervisor, Department of Physics

Acknowledgments

Since this thesis marks the culmination of my four years of undergraduate life here at MIT, I would like to take this opportunity to express my sincere gratitude for all those that have guided and supported me through this time.

First and foremost, I am gratefully indebt to my thesis advisor, Eric Hudson, without whom none of this would have been possible. I thank him for being there every step of the way, always ready and willing to answer my questions, even the most stupid and sometimes wacky ones, and always encouraging me to ask more. He has shown me what it means to be a good advisor and how to think like a physicist. Perhaps even more importantly, I thank him for introducing to me the joy of pursuing an area of physics research that I truly love, where fun and work become synonyms. And I thank him for giving me the opportunity to participate and fully apply myself as a contributing member in this field.

I would also like to thank my first research advisor, Gabriella Sciolla, who has given me unfaltering support and encouragement since day one, and even well after my project ended. Her dedicated working enthusiasm constantly inspires me to pursue my own path in physics. I cannot thank her enough for so patiently and encouragingly showing me, who was no more than a naive freshman back then, what it means to do physics research, and for instilling in me the drive to reach for and take advantage of the available opportunities around me.

This thesis would not have been possible without Mike Boyer, Doug Wise, and Kamalesh Chatterjee, the graduate students who have worked so laboriously and tenaciously to built the lab and the STM over the years from scratch. I thank them for all the lively discussions that make lab a fun place to be, ranging anywhere from physics to life in general.

I would be amiss if I didn't mention my friends who have shared my life these four years. I thank P and Y for always humoring me with my sudden bursts of often young-at-heart silliness, and constantly checking on each other's sanity balance against work. I thank Y especially for sharing with me all those all-nighters we've

pulled through the years, including those during the glorious days of junior lab.

Last but most importantly, I would like to thank my parents, who have always been there for me, to share my joy on sunny days and to encourage me on rainy days. I thank them for always believing in me even when I don't have the strength to do so myself. This thesis I dedicate to them.

Contents

1 Introduction **11**

1.1 Conventional Superconductivity 11

1.2 High Temperature Superconductivity 12

1.2.1 Doped Mott Insulators 13

1.2.2 Phase Diagram 13

2 Techniques and Materials **15**

2.1 Scanning Tunneling Microscopy 15

2.1.1 Topography 18

2.1.2 Spectroscopy 18

2.1.3 Spectral Survey 18

2.1.4 Temperature Dependence 19

2.2 Material 19

3 Energy Gaps **21**

3.1 Observed Gaps 22

3.1.1 Superconducting Gap 22

3.1.2 Pseudogap 24

3.2 Existing Theories on Gaps 24

3.2.1 Preformed Pairs 25

3.2.2 Competing Order 26

3.3 Existing Controversies 28

3.3.1 Smooth Evolution Through T_c 28

3.3.2 Spatial Inhomogeneity 29
3.4 Summary 29

4 STM Imaging of Two Gaps **31**
4.1 Data 31
4.2 Analysis 32

5 Significance of the Two Gaps **39**
5.1 Comparison with ARPES Results 40
5.2 Uniting STM Results 41
5.2.1 Smooth Evolution Through T_c 41
5.2.2 Nanoscale Inhomogeneity 41
5.2.3 Subgap Kink 42
5.3 Uniting Gap Theory 42
5.4 Future Experimental Directions 42

6 Conclusion **45**

A Data Processing Techniques **47**
A.1 Gap Finder 47
A.2 Warping 48

List of Figures

1-1 Simple high-T_c phase diagram 14

2-1 Schematic of an STM 16
2-2 Schematic of tip-sample tunneling 16
2-3 BSCCO crystal structures 20

3-1 Complex high-T_c phase diagrams 22
3-2 Comparison of s-wave and d-wave gaps 23
3-3 Example of a pseudogap 25
3-4 Smooth evolution of energy gap across T_c 27
3-5 Nanoscale inhomogeneity in Bi-2212 29

4-1 Topography and gap map of OD Bi-2201 sample 32
4-2 Temperature dependent comparison of spectra in OD Bi-2201 33
4-3 Gap maps of same region over a series of temperatures 34
4-4 Result of normalization on individual spectra 35
4-5 Gap map after normalization of spectral surveys 36
4-6 Temperature dependence of normalized small gap 37

Chapter 1

Introduction

Superconductivity is a phenomenon characterized by two properties: the complete vanishing of resistance below a critical temperature, T_c, and the expulsion of magnetic flux below a critical field H_c. It is itself a phenomenon of strongly correlated behavior in a many-body system, which is an important yet still unsolved mystery in physics today. As it stands, superconductivity is still a big puzzle with missing pieces. The whole range of intriguing and often surprising properties discovered in the field drives experimentalists to creatively find new missing pieces and to work together with theorists to complete the puzzle. The results are presented in this thesis with the hope that they would bring us one step closer to unveiling the beautiful picture that underlies the phenomenon of superconductivity.

1.1 Conventional Superconductivity

The first superconductor, Hg, discovered by K. Onnes in 1911 when he observed the sudden disappearance of resistance when cooled below 4K [1], was a conventional superconductor. Nearly half a century later, in 1957, Bardeen, Cooper, and Schrieffer put forth a microscopic quantum mechanical theory that succeeded in explaining the various experimental observations of superconductivity [2]. It became known as the BCS theory, and is now the universally accepted basis for describing superconductors.

The fundamental idea behind the BCS theory is that electrons in the material

form pairs, known as Cooper pairs, through phonon coupling. In a somewhat simplified picture, negative charge of a conducting electron slightly distorts the lattice, temporarily creating a higher concentration of positive charge that in turn attracts a second electron, coupling the two electrons. This pairing occurs between electrons of equal and opposite momentum, and is favored when the potential energy lowered due to this process is greater than the Coulomb repulsion between the pairing electrons. When the material is cooled below a critical temperature, these Cooper pairs condense into a single coherent ground state, and move through the crystal without scattering, superconducting. The pairing model is consistent with the experimental observation that the density of states of superconducting materials is gapped at the Fermi surface.

1.2 High Temperature Superconductivity

A whole new class of superconductors was discovered when Bednorz and Müller observed superconductivity in $La_{2-x}Ba_xCuO_4$, with a T_c of 38K, followed by materials that were found to superconduct at above-liquid nitrogen temperatures such as $YB_2C_3O_{6+x}$ with a T_c of 95K, and $Bi_2Sr_2CaCu_2O_{8+\delta}$ with a T_c of 92K. This new class became known as the high temperature superconductors (HTSC). Aside from having T_c much higher than conventional superconductors, these oxide superconductors are all Perovskite (layered) systems with weakly coupled planes in which the coherence length in the direction perpendicular to the planes are much smaller than the interlayer separations, making them effectively 2D systems. Moreover, all these materials have copper oxide planes in their crystal structures, and are referred to as the cuprates. Like conventional superconductors, the fundamental conducting charge in HTSC is still observed to be 2e, suggesting that some sort of pairing is still at play, even though the nature of the pairing mechanism is still uncertain. Unlike conventional superconductivity, there are still numerous properties of HTSC for which the BCS theory fails to account, and there has not yet been a universally accepted theory that unites all experimental facts about HTSC. Interpretations of experimental

results of HTSC are under constant debate.

1.2.1 Doped Mott Insulators

One of the most surprising properties of these high-T_c cuprates is that, contrary to conventional superconductors, the parent compounds of cuprates are all insulators, more specifically, they are all antiferromagnetic Mott insulators, and become superconducting only with doping. Since the common feature among all high-T_c cuprates is the copper oxide planes, these planes are thought to be linked to the phenomenon of superconductivity in these materials.

Shortly after the 1986 discovery of HTSC, P. Anderson summarized the properties of the new superconductors by drawing out three essential features that they share. First, the materials are quasi-two-dimensional, with the CuO_2 plane as the key structural unit. Second, high-T_c superconductivity is created by doping a Mott insulator. Third, the combination of the first two features would result in fundamentally new behavior that is inexplicable in terms of conventional metal physics [3].

A Mott insulator is fundamentally different from a conventional insulator. In a conventional insulator, the highest-occupied band is entirely filled with two electrons per unit cell. Conductivity is prohibited by the Pauli exclusion principle. In a Mott insulator, the valence band is only half-filled, with one electron per unit cell. However, conductivity is still prohibited because Coulomb repulsion is strong enough to block a second electron from occupying any unit cell. With doping, which is adding charge carriers to the material, conductivity can be restored in a Mott insulator [3].

1.2.2 Phase Diagram

Both temperature and doping level play critical roles in determining the state of a high-T_c cuprate. Fig. 1-1 shows a typical phase diagram of cuprates parameterized by these two factors. The horizontal axis is hole doping level. At low doping, the material is an anti-ferromagnetic insulator (AF). As dopant level increases, the material becomes superconducting within the dome-like feature (SC). At high dopant level,

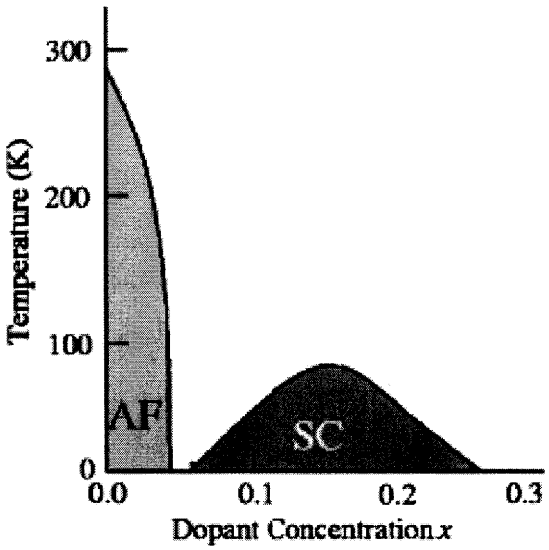

Figure 1-1: Typical phase diagram of high temperature superconductor parametrized by doping and temperature.

the material again becomes nonsuperconducting. The lack of explanation for this doping-dependence in HTSC is one of the reasons that the BCS theory is inadequate for HTSC.

The vertical axis is temperature. Just like conventional superconductors, superconductivity is killed when warmed above a critical temperature, T_c, which, in the phase diagram, is marked by the roof of the SC dome at different dopant levels. The dopant level that gives the highest T_c is called optimal doping. Materials with lower dopant levels are referred to as under-doped and those with higher dopant levels over-doped.

The picture of HTSC is not well understood, both experimentally and theoretically. The phase diagram I show here has the most basic structures that are universally accepted for all high-T_c cuprates. The region beyond the AF and SC regions is even less understood and agreed upon. There exists a plethora of theories, each of which has its own complexity built upon the basic phase diagram, especially in the region beyond the SC dome. We shall come back to a more detailed discussion of this region in light of the available theories in Ch. 3.

Chapter 2

Techniques and Materials

All results presented in this thesis are obtained using a specially designed temperature dependent scanning tunneling microscope (STM) on the material Pb-$Bi_2Sr_2CuO_{6+\delta}$. In this chapter, I shall briefly introduce both the technique of STM and the material used.

2.1 Scanning Tunneling Microscopy

The technique of scannning tunneling microscopy (STM) was developed in 1982 by Binnig and Rohrer[4], who received the Nobel Prize in Physics for this work in 1986. STM is built upon the quantum mechanical phenomenon of tunneling. The basic principle of operation of an STM, as shown in Fig. 2-1, consists of holding an atomically sharp conducting tip above a flat conducting sample. When a bias voltage is applied between the tip and the sample, electrons tunnel through the vacuum barrier, forming a measurable tunneling current, which is dependent on both the tip-sample separation as well as the availability of electronic states in the sample at the tip position. Biasing the sample by a negative voltage -V relative to the tip effectively raises the Fermi level of the sample electrons relative to the electrons in the tip, shown in Fig. 2-2.

Intuitively, the tunneling current from the sample to the tip must be proportional to three factors, the tunneling probability $|M|^2$, the number of filled sample states

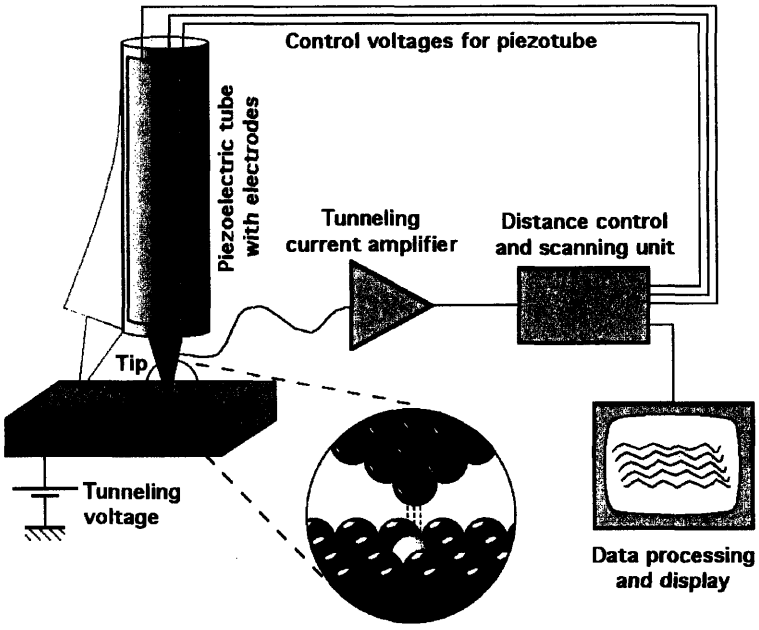

Figure 2-1: Schematic of an STM: When the tip is brought close to the sample, a bias voltage between the tip and the sample causes electrons to tunnel through the vacuum barrier, forming a measurable tunneling current that depends on the tip-sample separation as well as the electronic properties of the sample at the tip position.

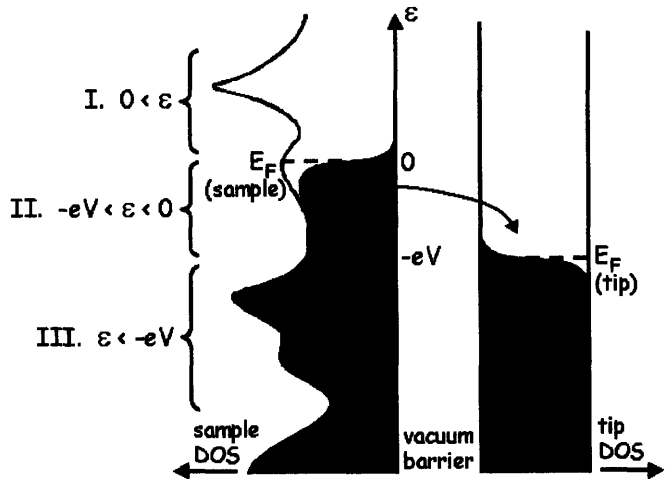

Figure 2-2: Schematic of tip-sample tunneling: vertical axis shows energy, horizontal axis is density of states (DOS) of both the sample and the tip. States are filled up to the Fermi level. In operation, a bias voltage between the tip and sample effectively offsets the Fermi levels, allowing electrons to tunnel from the filled higher energy states to the empty lower energy states across the vacuum barrier. In this drawing, a negative bias is applied to the sample, raising its Fermi level and causing a measurable net tunneling current to flow from the sample to the tip.

to tunneling from, and the number of empty tip states to tunnel into. When also taking into account the reverse current from the tip to the sample, we have the total tunneling current:

$$I = -\frac{4\pi e}{\hbar}\int_{-\infty}^{\infty}|M|^2\rho_s(\epsilon)\rho_t(\epsilon+eV)\{f(\epsilon)[1-f(\epsilon+eV)]-[1-f(\epsilon)]f(\epsilon+eV)\}d\epsilon, \tag{2.1}$$

where we have taken ϵ=0 to be the Fermi energy, $\rho_{t(s)}$ is the density of state of the tip(sample), and f(ϵ) is the Fermi function:

$$f(\epsilon) = \frac{1}{1+e^{\epsilon/k_BT}}. \tag{2.2}$$

The expression for the tunneling current can be simplified in several ways. First of all, we use a normal conducting metal for the tip, which has a constant density of states, $\rho_t = \rho_t(0)$. In addition, our STM is operated at low temperatures for the measurements documented in this thesis, we can thus approximate the Fermi function as a step function. Using the WKB approximation by treating the vacuum between the tip and sample as a square barrier, the tunneling probability can be shown to have a simple exponential dependence on the tip-sample separation. After all simplification, the total tunneling current becomes [5]

$$I \approx \frac{4\pi e}{\hbar}e^{-s\sqrt{\frac{8m\psi}{\hbar^2}}}\rho_t(0)\int_{-eV}^{0}\rho_s(\epsilon)d\epsilon, \tag{2.3}$$

where s is the tip-sample separation, ψ is directly related to the the work functions of the tip and sample, and V in the lower integral limit is the bias voltage.

Because the DOS is a function of the locatioin of the tip as well as the bias voltage applied, we can extract from the tunneling current a host of information about the sample, making STM a powerful technique for atomically resolved spatial imaging and spectroscopy of superconducting materials.

2.1.1 Topography

One of the most basic modes of operation of STM is constant-current mode. When scanning the tip across the sample, we use a feedback system to hold the tunneling current constant by adjusting the vertical position of the tip. Because of the exponentially sensitive dependence of the tunneling current on the tip-sample separation, holding the current constant is effectively equivalent to holding the tip and sample separation constant. Then from the adjustment of the vertical height of the tip needed to keep the current constant, we can map out the topography of the sample surface.

2.1.2 Spectroscopy

In Eq. 2.3, we see that the tunneling current is proportional to the integrated DOS. The derivative of the current then is proportional to the DOS directly. We call this dI/dV the conductance $g(V)$,

$$g(V) = \frac{dI}{dV} \propto DOS(eV), \tag{2.4}$$

which we measure directly using a standard lock-in amplifier.

Rather than scanning over the sample surface as in topographical measurements, we can park our STM tip at a certain location. By varying the DC bias voltage and applying a small voltage modulation using a lock-in, we can measure the DOS of the sample at the tip position as a function of bias voltage.

2.1.3 Spectral Survey

We can also combine the techniques of topography and spectroscopy by scanning across the sample surface and measuring DOS at a dense array of locations, which we call a spectral survey. This allows the mapping of spatial variations of spectral features. Such surveys have led to the direct visualization of atomic scale effects, such as single atom impurities [6, 7] and oxygen dopant atoms [8]. Key results documented in this thesis were obtained using spectral surveys.

2.1.4 Temperature Dependence

In addition to the standard measurement ability described above, our STM has the specially designed ability to do temperature dependent measurements, that is, we are able to follow a spatial region of the sample atom by atom and take measurement at a range of temperatures down to 4K with sub-millikevin stability. We are the first to achieve this. This ability is crucial to the developement of the analytical technique documented in this thesis. By doing spectral surveys of the same region at a range of temperatures, we are able to observe variations of spectral features as a function of both space and temperature.

2.2 Material

The high-T_c cuprates fall mainly into three major families of compounds: $La_{2-x}Sr_xCuO_4$ (LSCO), $YBa_2Cu_3O_{6+x}$ (YBCO), and $Bi_2Sr_2CaCu_2O_{8+\delta}$ (BSCCO). The third family, BSCCO, cleaves easily in vacuum due to the weak bonds between its BiO layers, resulting in atomically flat surfaces, which makes it an ideal compound to be studied using an STM. Fig. 2-3 shows the crystal structures of two members of this family. Within this family, extensive work has been done on $Bi_2Sr_2CaCu_2O_{8+\delta}$, or Bi-2212 (Fig. 2-3(a)), which has two copper oxide planes and a T_c of 92K at optimal doping. The material used for work documented in this thesis were done on Pb-$Bi_2Sr_2CuO_{6+\delta}$, or lead doped Bi-2201, with a single copper oxide plane instead of two (Fig. 2-3(b)). Bi-2201 is observed experimentally to be more inhomogeneous than Bi-2212. Also, Bi-2201 has a much lower T_c of 35K at optimal doping compared to Bi-2212 (T_c=92K), hence a smaller superconducting dome in the phase diagram.

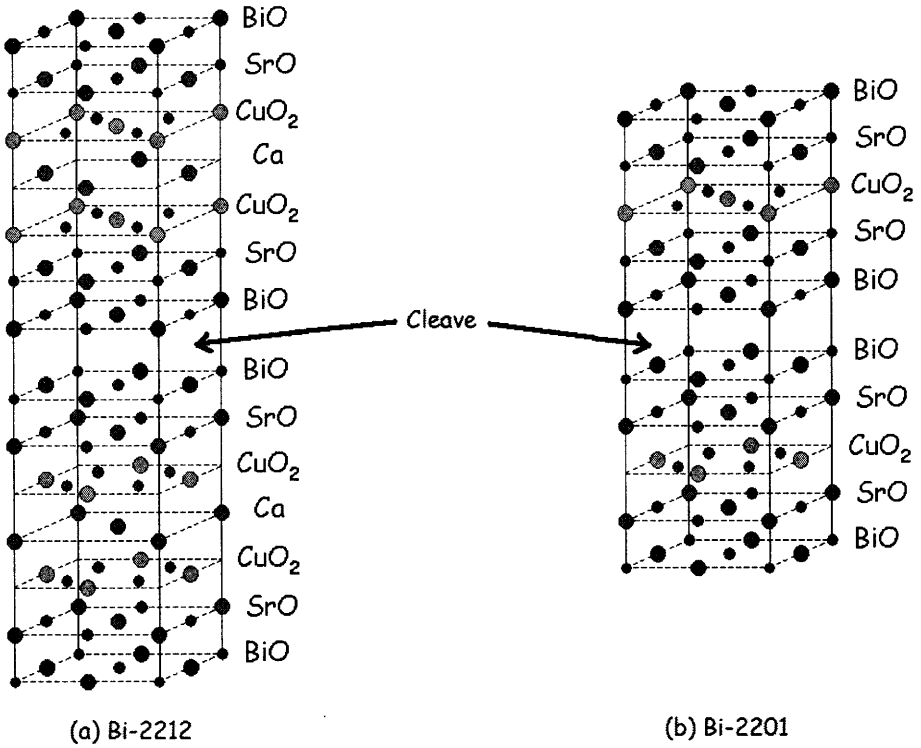

Figure 2-3: (a) Structure of $Bi_2Sr_2CaCu_2O_{8+\delta}$ (Bi-2212), with two copper oxide planes. (b) Structure of $Bi_2Sr_2CuO_{6+\delta}$ (Bi-2201), with only one copper oxide. Materials in the BSCCO family are easily cleaved due to the weak bonds between the BiO planes.

Chapter 3

Energy Gaps

A gapped density of states at the Fermi surface is a signature feature for all types of superconducting materials. In conventional superconductors, this gap feature is explained via pairing, and vanishes at T_c, above which the material no longer superconducts. For HTSC, the spectroscopic picture is not as simple. While a gap still exists below T_c, the DOS is observed to be gapped well above T_c as well. This gap above T_c is commonly referred to as the pseudogap (Fig 3-1(a)). The pseudogap phase is not a well-defined phase, since a definite finite-temperature phase boundary has never been found. The line drawn in the figure only serves as a guide to the crossover region. The observable presence of pseudogap in the underdoped region is more pronounced than in the overdoped region. The exact behavior of this crossover line in the overdoped region relative to the superconducting dome is still under debate. Because the pseudogap is the phase high-T_c cuprates transition into when superconductivity vanishes at T_c, there has been an immense interest in the HTSC community to understand the nature of the pseudogap and its possible relation to the phenomenon of HTSC in the hope of understanding the phenomenon of HTSC itself.

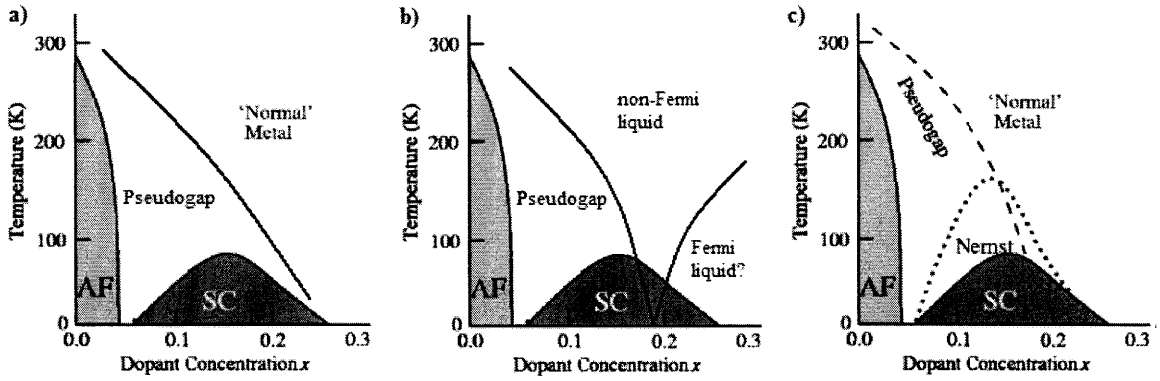

Figure 3-1: Phase diagrams of high-T_c cuprates in light of dominant theories showing various regions: (a)Phase diagram including a pseudogap phase above the superconducting dome, with a crossover region into the "normal" metal state. (b)Phase diagram showing the inclusion of a quantum critical point below the SC dome. (c)Phase diagram showing the Nernst region where vortices are observed above T_c, suggestive of a competing order to superconductivity.

3.1 Observed Gaps

3.1.1 Superconducting Gap

We refer to the gap occuring below T_c as the superconducting gap. Many measurements have shown that the superconducting gap in conventional superconductors differs from that in HTSC. Conventional superconductors are s-wave, that is, the gap magnitude is isotropic in momentum space (Fig. 3-2(a)). Under BCS theory, the DOS of an s-wave superconductor is

$$DOS(\epsilon_k) = \begin{cases} \frac{\epsilon_k}{\sqrt{\epsilon_k^2 - \Delta^2}} & \epsilon_k > \Delta \\ 0 & \epsilon_k < \Delta \end{cases}, \tag{3.1}$$

where Δ is the gap magnitude, independent of angle. The gap that an STM measures is an integrated average over the angle in momentum space. Fig. 3-2(b) shows such an integrated gap, while Fig. 3-2(c) shows real STM data on a conventional superconductor $NbSe_2$.

Unlike conventional superconductors, high-T_c superconducting gaps are d-wave, with an angle-dependent gap magnitude (Fig. 3-2(d)). The angle dependence of the

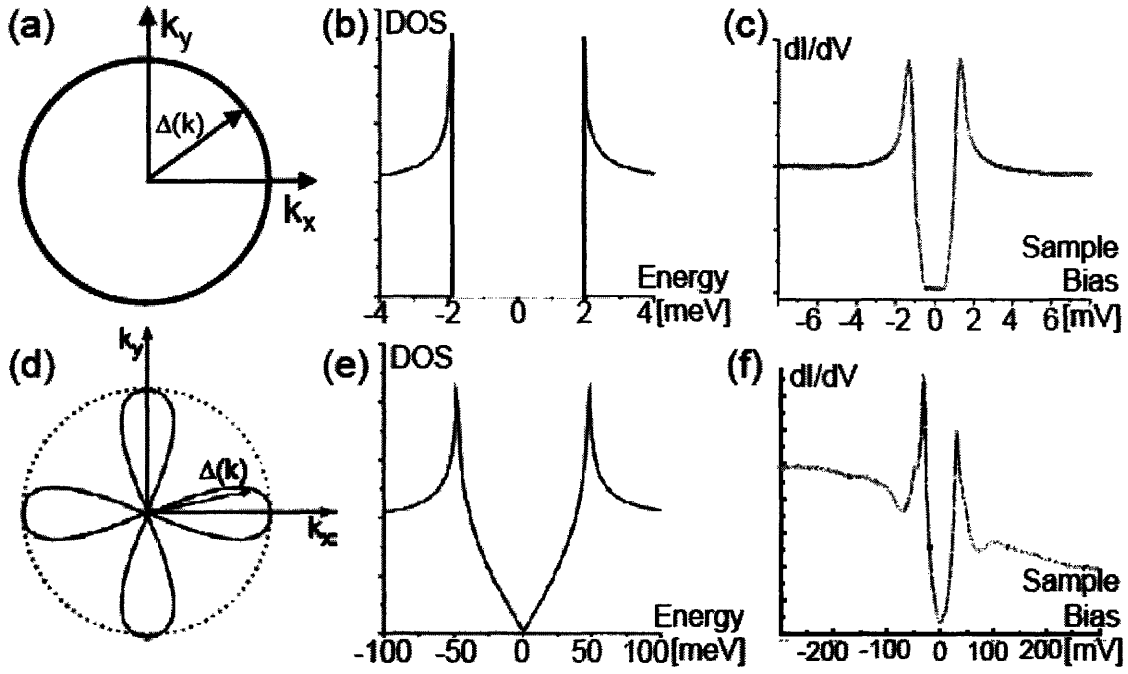

Figure 3-2: Comparison of s-wave and d-wave gaps [5]: (a) Gap magnitude is isotropic in momentum space for an s-wave superconductor. (b) Averaged gap integrated over angle in moment space for an s-wave superconductor. (c) Actual superconducting gap measured by an STM in the conventional superconductor, $NbSe_2$. (d) Gap magnitude is angle-dependent for a d-wave superconductor. (e) Averaged gap integrated over angle in momentum space for a d-wave superconductor, showing the V-shape feature. (f) Actual superconducting gap measured by an STM in the HTSC BSCCO.

gap opening is observed to follow a cosine relation, $\Delta(\theta_k) = \Delta_0 \cos(2\theta_k)$, which has a four-fold symmetry in momentum space. The integrated gap that an STM measures for such an angle-dependence is a V-shaped gap since it is an average of gaps of varying sizes. Fig. 3-2(e) and (f) show examples of calculated gap and real data on Bi-2212, respectively. A common feature in the superconducting gaps in both conventional and high temperature superconductors are the two peaks on either side of the gap. These are commonly referred to as the "coherence peaks." Since BCS is not an adequate theory for high-T_c cuprates, Eq. 3.1 is no longer a necessarily adequate expression for the DOS, and there is not yet an accepted theory for HTSC. Since the gap magnitude Δ is strictly defined by a fitting function, we do not have a way to associate it with the observed high-T_c gap. Instead, experimentally we choose to define Δ as half the distance between the peaks around the measured gap.

3.1.2 Pseudogap

Different from conventional superconductors, a gap is found to exist above T_c in HTSC, and is qualitatively different from the superconducting gap below T_c. The lack of explanation for this pseudogap is another reason that the BCS theory fails to describe HTSC. Fig. 3-3 shows an example of a pseudogap observed in Pb-$Bi_2Sr_2CuO_{6+\delta}$. Within the same sample, pseudogap is typically much wider than the superconducting gap. Also, compared to the superconducting gap, the peaks around the pseudogap are typically strongly suppressed.

3.2 Existing Theories on Gaps

The intriguing complexity in the high-T_c cuprates revealed through the multitude of measurements over the years has contributed greatly to the outpouring of a myriad of theories for HTSC. Currently, the HTSC community stands between two major camps regarding the relation between the superconducting gap and the pseudogap.

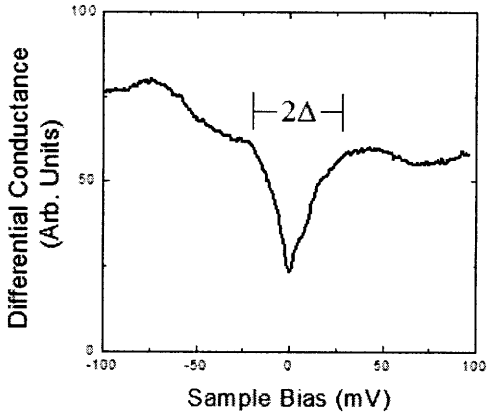

Figure 3-3: STM measurement of a pseudogap observed in $Bi_2Sr_2CuO_{6+\delta}$. The gap magnitude, Δ, is defined as half the gap opening.

3.2.1 Preformed Pairs

One of the earliest theoretical attempts on HTSC was the "resonating valence bond" (RVB) theory put forth by Anderson [9]. This attempt perhaps grew out of the effort to work the role of doping into the BCS framework. The fundamental idea is that virtual charge fluctuations in a Mott insulator lead to a long-range antiferromagnetic order. The quantum fluctuations in a 2D spin-$\frac{1}{2}$ system such as the CuO_2 plane in the cuprates, however, are somehow strong enough to destroy the long-range spin order, resulting in a "spin liquid" which contains electron pairs whose spins are locked in a singlet configuration. These pairs resemble the Cooper pairs in conventional superconductors, and would become free to conduct when average occupancy is lowered by doping. Under this theory, the superconducting pairs in the system are pre-formed in the normal state, thus the pseudogap is the continuation of the superconducting gap into the non-phase coherent regime.

However, it was soon discovered experimentally that the spin liquid is not realized in the underdoped cuprates. In the underdoped region above T_c in the phase diagram, behavior of non-Fermi liquid were observed, such as the resistivity being linear in T and the Hall coefficient being temperature dependent [10]. This suggested the addition of a quantum critical point under the superconducting dome to the phase

diagram (Fig. 3-1(b)) [11, 12, 13].

Even though RVB is not completely right, the idea that there is a single pairing gap in the system is still one of the dominant beliefs in the HTSC community. The basic underlying idea is that the pseudogap above T_c is the precursor of the superconducting gap below T_c. In other words, the pseudogap and the superconducting gap are the same gap. Electron pairs are formed at temperatures above T_c, but phase coherence only sets in at T_c, enabling superconductivity [9, 14, 15, 16, 17, 18, 19].

One suggestion for the mechanism that onsets phase coherence is phase fluctuation [16]. The idea is that superconductivity depends on two energy scales in the system, the pairing amplitude, Δ, which measures the strength of the binding energy of the Cooper pairs, and the phase stiffness, ρ_s, which measures the ability of the superconducting state to carry a supercurrent. In conventional superconductors, Δ is much smaller than ρ_s, hence the breaking of Cooper pairs destroys superconductivity. In HTSC, however, the two energy scales are on the same order, especially in the underdoped region, where ρ_s could be weaker, and therefore it would be ρ_s rather than Δ that determines the onset of superconductivity [16, 3, 13].

The major piece of experimental evidence supporting this one-gap hypothesis is spatially averaged temperature-dependent STM measurements of underdoped Bi-2212 by Renner *et al* [20], shown in Fig. 3-4. First of all, there is clear existence of a gap at T_c, contrary to conventional superconductors in which the gap closes completely at T_c. Secondly, the gap in Bi-2212 seems to evolve smoothly from below T_c to above T_c, with the same energy scale. These trends were also observed in Bi-2212 of other doping levels [20, 21] and Bi-2201 [22]. In addition, the gap above T_c observed in these systems seem to scale with the gap below T_c across doping levels [23]. These trends have led to the interpretation of the observed gap below and above T_c as the same gap.

3.2.2 Competing Order

An alternative interpretation of the pseudogap is that it is an order that competes with superconductivity. In order to present the theories of competing orders, we must

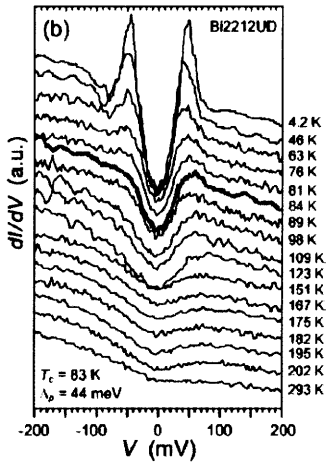

Figure 3-4: Spatially averaged temperature-dependent STM measurement of the energy gap across T_c in underdoped Bi-2212 with T_c=83K, showing a smooth evolution of the gap across T_c [20].

first introduce two phenomena: magnetic vortices and the Nernst effect.

Superconductors expel magnetic field up to some critical field strength, after which the magnetic flux punctures through in small bundles, creating vortices in the superconductor. Within these vortices, superconductivity is killed. The density of the vortices increases as the external magnetic field is increased until at another critical field strength superconductivity is completely killed.

Nernst effect is the phenomenon that when a flow of vortices is induced in a superconductor, an electric field appears transverse to the flow direction because of Josephson effect. Measurement of the Nernst effect is a sensitive measurement of the presence of vortices, and has been used to show the existence of vortices above T_c, resulting in a phase diagram with the added "Nernst region" above the superconducting dome for underdoped cuprates (Fig. 3-1(c)) [24, 13].

Within the vortex core, pairing amplitude vanishes. Yet, STM measurements have shown that an energy gap exists within vortex cores [25, 26]. This means that the gapped state in the vortex cores is not due to the pairing mechanism used to describe the superconducting gap below T_c. There are *two* gaps in the system. Moreover, the observation of vortices above T_c, i.e. in the Nernst region, suggests that the gap phase in the vortex cores is a competing order to rather than a continuation of the

superconducting phase below T_c [13].

A number of theories have been proposed to explain the competing orders. The SO(5) model by S.-C. Zhang is based on the idea that the the core has an antiferromagnetic order [27]. Another proposal is orbital currents, where the competing order persists in the pseudogap region but is hidden from detection because of the difficulties of coupling to the order [11, 28].

3.3 Existing Controversies

Perhaps the reason there has not yet been a comprehensive theory for HTSC is that the interpretation of the wealth of experimental results on HTSC is still far from being united. There are two major controversies plaguing the interpretation of STM results that we focus on in this thesis.

3.3.1 Smooth Evolution Through T_c

As examplified by the temperature dependent STM spectroscopy data shown in Fig. 3-4, many groups observe a smooth evolution of the gap in the DOS from the superconducting state to the pseudogap state across T_c. The lack of any apparent sudden change in the DOS at T_c does not fare well with the fact that superconductivity is a phenomenon with a measurable and definite transition temperature. Moreover, under the single gap hypothesis, these results conflict with other types of measurements. Deutscher, for example, has shown that the gap measured by STM and angle-resolved photoemission spectroscopy (ARPES) is different from the gap measured by Andreev reflection, penetration depth and Raman spectroscopy, and thus that there are two distinct energy scales in the system [29]. Even Nernst effect studies which, like STM, find a smooth thermal evolution (here indicating the presence of vortex fluctuations above T_c) do find an onset temperature which scales with T_c [24], rather than simply decreasing linearly with doping as the tunneling measured gap does [30].

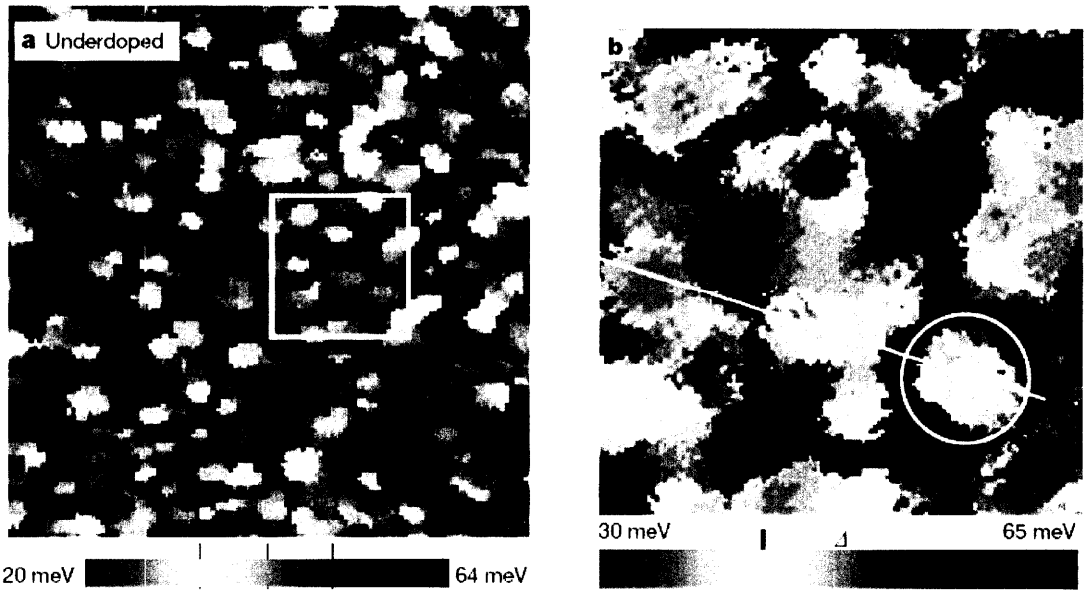

Figure 3-5: First published gap map made from STM spectral survey on underdoped Bi-2212 sample with T_c=79K, showing nanoscale inhomogeneity, taken at 4.2K. (a) Gap map of an area of $560\mathring{A} \times 560\mathring{A}$. The color scale means a gap range of 20-64meV. (b) Gap map generated from a spectral survey of the $147\mathring{A} \times 147\mathring{A}$ region in the white box in (a).

3.3.2 Spatial Inhomogeneity

Another controversial result is nanoscale inhomogeneity, in which gap magnitudes are observed to vary wildly on nanometer length scales [31, 32, 33, 34, 8]. To study inhomogeneity we can extract from spectral survey a gap map $\Delta(\vec{r})$, where the gap magnitude Δ is mapped spatially. Fig. 3-5 shows the first published gap map by Lang *et al*, showing nanoscale inhomogeneity in Bi-2212 revealed by an STM. However, large superconducting gap variations on short length scales are inconsistent with NMR and heat capacity data [35].

3.4 Summary

Ever since the realization of the existence of a gap above T_c, the pseudogap, that marks HTSC different from conventional superconductors, the effort to understand the pseudogap and its relation to superconductivity has been a major focus of HTSC

research, both experimentally and theoretically. The advent of STM has undoubtedly made great contributions to the experimental picture of HTSC, however, it has also introduced troubling controversies, including the apparent smooth transition of the gap across T_c and nanoscale inhomogeneity. The difficulty in interpretating these controversial results also played a major part in keeping the theoretical picture of HTSC divided under either the preformed pair hypothesis or the competing order hypothesis. Experimentally establishing the number of gaps in the system is clearly the pressing issue at hand in uniting and advancing HTSC research.

Chapter 4

STM Imaging of Two Gaps

The material we studied was Pb-$Bi_2Sr_2CuO_{6+\delta}$, or lead-doped Bi-2201. The sample was overdoped with a T_c of 15K. We have taken spectral surveys at a series of temperatures across its T_c.

The sample was cleaved at the BiO plane in cryogenic ultra high vacuum. All spectra reported here were measured under the same settings: $V_{sample} = -100mV$, $I = 100pA$, and $V_{mod,rms} = 1.6mV$. Several techniques were developed in processing raw data in preparation for analysis, all documented in Appendix A.

4.1 Data

Fig. 4-1(a) is a topograhy of the region under study, with an area of $180\mathring{A} \times 180\mathring{A}$, clearly showing the resolved atomic lattice of the BiO plane. The brighter atoms are the Bi-replaced Pb atoms, confirmed by comparing its concentration with the expected Pb doping level of 0.38 in the sample. We observe no correlation between spectroscopy and the presence or absence of Pb atoms. Fig. 4-1(b) is the gap map, $\Delta(\vec{\mathbf{r}})$, made from a spectral survey taken over the region at T=6K. Consistent with previous STM measurements [32], we see nanoscale inhomogeneity in the gap distribution. Another way to present the spectral variations in the material is shown in Fig. 4-1(c), where a set of spectra extracted from the spectral survey is plotted, with gap sizes varying from 7meV to 40meV.

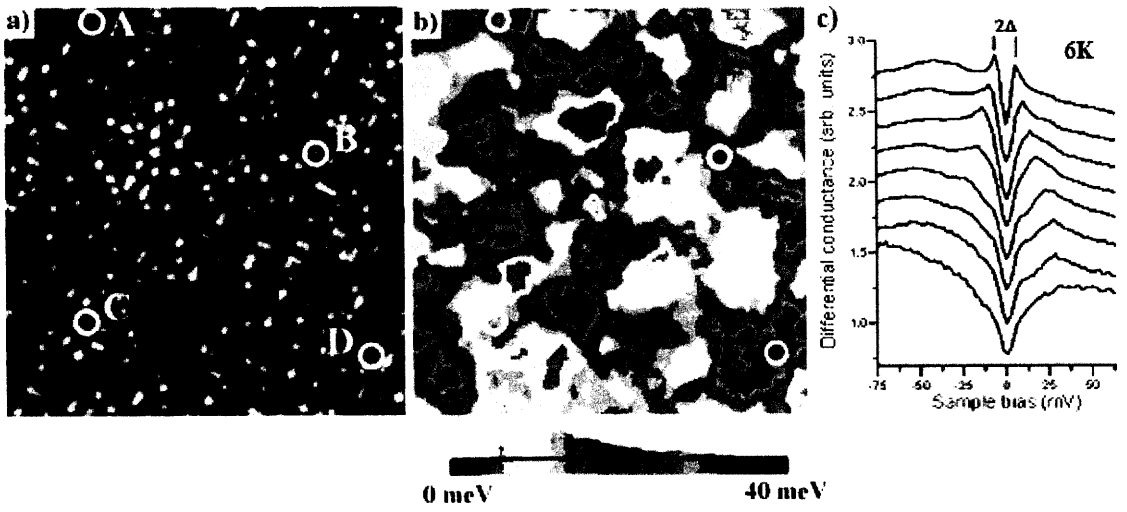

Figure 4-1: (a) Topographical image of a single $180\mathring{A} \times 180\mathring{A}$ field of view of overdoped Pb-Bi-2201, clearly showing the resolved atomic lattice of the cleaved BiO plane. The brighter atoms are the Pb atoms, which have shown no observable spectral effect. (b) Gap map, $\Delta(\vec{r})$, made from a spectral survey taken over the same region at T=6K. The color scale below shows a gap variation ranging from 0meV to 40meV. (c) A set of spectra associated with gap values ranging from Δ=7meV to 40meV, extracted from the spectral survey, showing the scope of spectral variation in the region. The spectra are offset vertically to enhance visibility.

We also made temperature dependent spectral measurements, plotted in Fig. 4-2. Consistent with previous STM measurements [20], we observe a smooth evolution of the gap from below T_c to above T_c.

In addition to the results obtained using standard techniques introduced in previous STM work presented above, we were the first to be able to do spectral surveys on the same region at a series of temperatures, and make a gap map at each temperature to study gap variation as a function of space and temperature simultaneously. Fig. 4-3 shows such a series of gap maps made on overdoped Bi-2201.

4.2 Analysis

The nanoscale inhomogeneity is apparent in each gap map in Fig. 4-3. But strikingly, this inhomogeneity is almost entirely temperature-independent, even when warmed through T_c=15K. That is, in the pictured region, over fifteen thousand widely varying

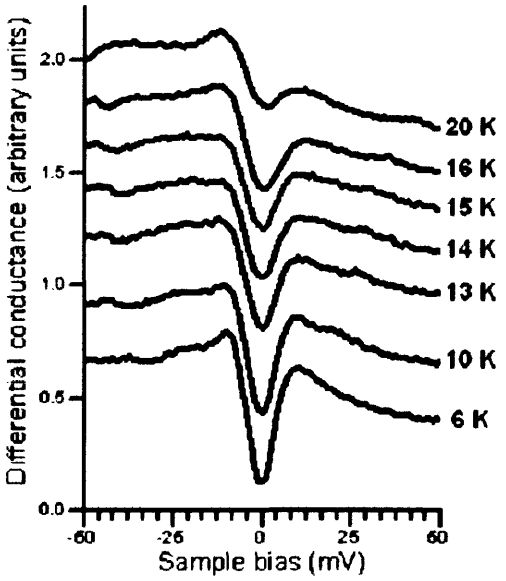

Figure 4-2: Spectra measurements taken at a series of temperatures for the overdoped Bi-2201 sample, showing a smooth evolution of the gap across T_c=15K, marked in red.

spectra evolve smoothly with temperature, apparently disregarding the superconducting transition at T_c, and thus preserving the initial gap width inhomogeneity. Since we know that superconductivity is a phenomenon that is highly sensitive to T_c, the independence of inhomogeneity in the sample on temperature must mean that inhomogeneity has little, if at all, to do with superconductivity. The question then becomes, what does?

To find the spectral change that actually took place at the onset of superconductivity at T_c, we go back to the spectra in the survey from which the gap maps were made and remove the effective background of the high temperature spectra from the low temperature ones. We thus calculate a normalized differential conductance G_N as a function of energy E, position $\vec{r}$, and temperature T by the common technique of dividing out the background, in this case a spectrum from the same position at a higher "normalization temperature" $T_N > T_C$:

$$G_N(E, \vec{r}, T) = \frac{G(E, \vec{r}, T)}{G(E, \vec{r}, T_N)}. \tag{4.1}$$

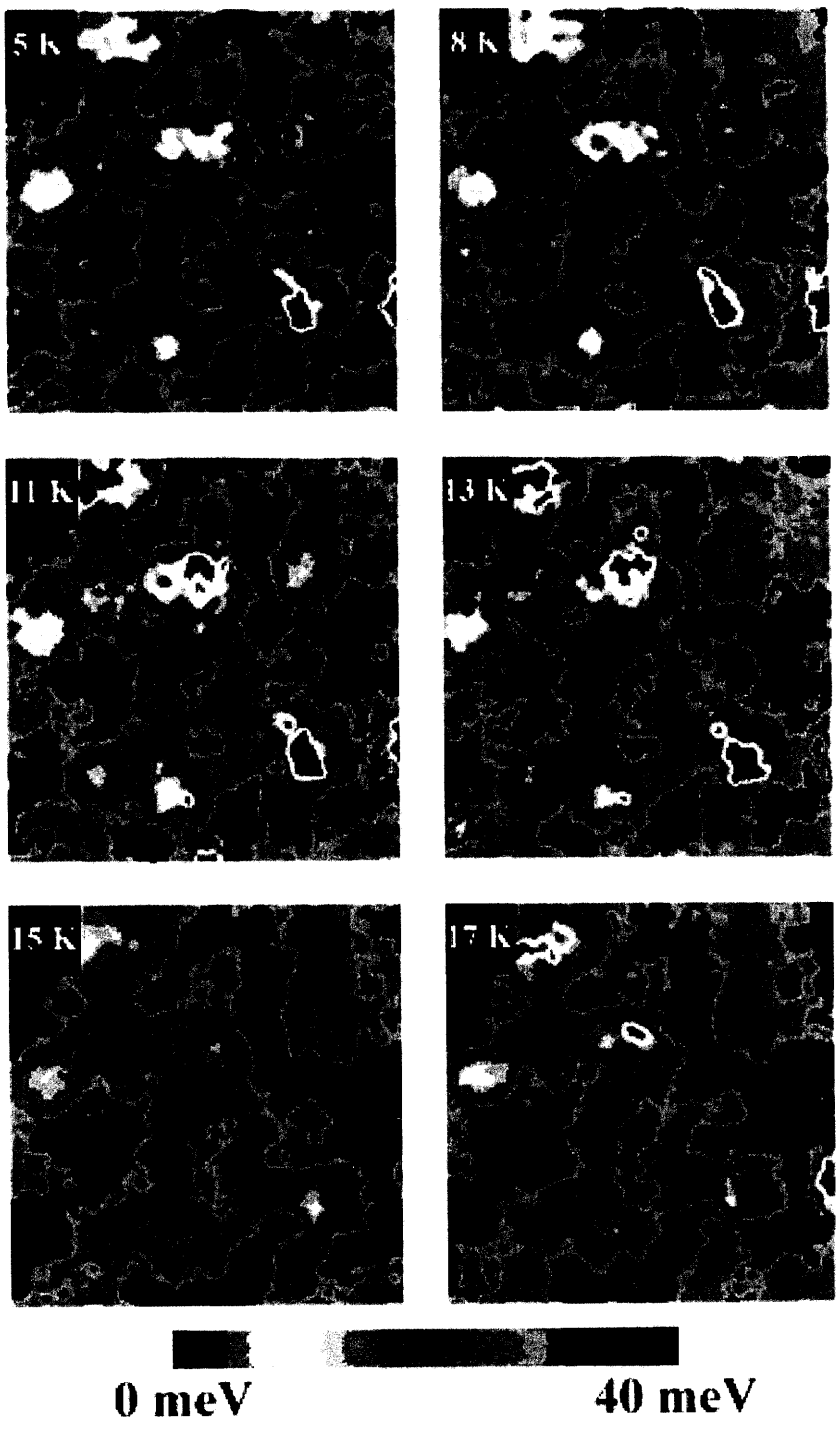

Figure 4-3: Gap maps made from spectral surveys of the same $175\mathring{A} \times 175\mathring{A}$ region on an overdoped Bi-2201 sample of T_c=15K, at a range of temperatures: T=5K, 8K, 11K, 13K, 15K, and 17K. All gap maps share the same color bar.

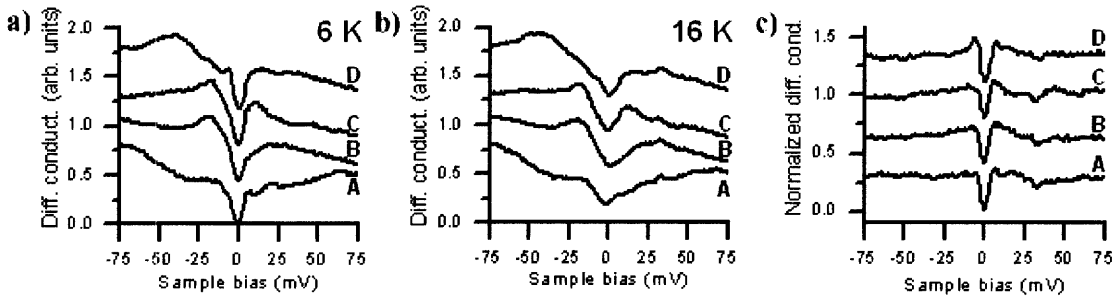

Figure 4-4: (a,b) Individual spectra taken at the four locations identified in Fig. 4-1 at T=6K and 16K respectively, representative of the wide spectral variation across the samples. (c) Normalized spectra $G_N = \frac{G(6K)}{G(16K)}$ of the same locations. Note that all high energy variation is removed, leaving a small, consistent gap.

We use division here for two reasons. First, it is often the correct normalization scheme, as, for example, in conventional (BCS) superconductors where the onset of superconductivity creates a superconducting density of states N_S by opening a gap which multiplies the normal state density of states N_0:

$$N_S \approx N_0 \frac{|E|}{\sqrt{E^2 - \Delta^2}}. \tag{4.2}$$

By dividing, we treat the temperature independent part of the spectra as the normal state of density, which is reasonable in the temperature range we are concerned with. Second, other normalization schemes, such as subtraction, are difficult given that STM measured differential conductance is only proportional to the density of states, where the constant of proportionality is unknown as well as temperature and position dependent.

We show the result of this normalization on several distinct spectra in Fig. 4-4. The locations of these spectra are marked in Fig. 4-1. Fig. 4-4(a) and (b) show the spectra taken at those four points at 6K and 16K, respectively, indicative of the widely varying spectra observed across these samples. After division, the temperature independent, inhomogeneous gap is removed and we find that a small gap remains, shown in Fig. 4-4(c).

Now applying the same normalization technique to every one of the more than fifteen thousand spectra in the entire survey behind the gap map of Fig. 4-1(b) demon-

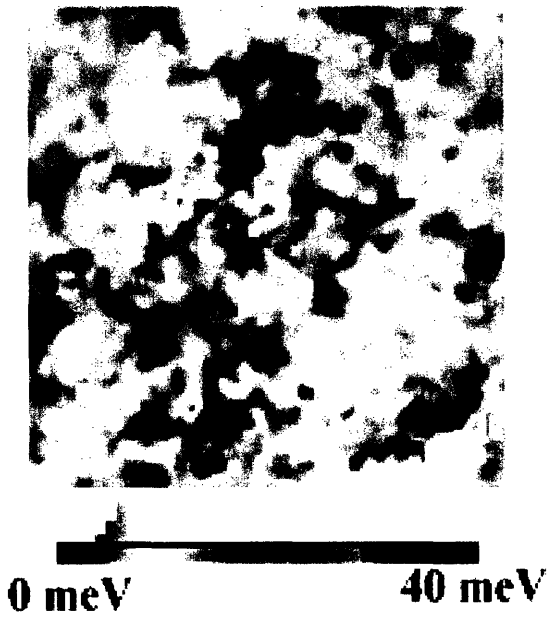

Figure 4-5: Gap map made after normalization of the spectral survey taken at 6K by the spectral survey taken over the same region at 16K, showing significantly increased homogeneity ($\Delta_N = 6.7 \pm 1.6meV$). The small remaining Δ_N variations show no correlation with Δ_{6K} or Δ_{16K}.

strates that this small gap is present throughout the sample, and is significantly more homogeneous than the larger gap we normalized away (Fig. 4-5). The mean and standard deviation of measured gap magnitudes (Fig. 4-1(b) and Fig. 4-5) drop from $\Delta_{large} = 16 \pm 8meV$ to $\Delta_{small} = 6.7 \pm 1.6meV$.

Not only is this newly revealed small gap homogeneous, it must also have a different temperature dependence than the large gap that we normalized away for this normalization scheme to successfully produce this result. In order to clarify this, we plot (Fig. 4-6(a)) the average of normalized (T_N=17K) spectral surveys at several temperatures below T_c=15 K. In contrast to the apparent temperature independence of the unnormalized spectra, we find that the normalized spectra are strongly temperature dependent, with the small gap vanishing near T_c.

One might protest that by choosing a normalization temperature T_N close to T_c we enforce this disappearance of the small gap. After all, $G_N(T = T_N)$ must be a straight line. In fact, the above results are relatively insensitive to our choice of T_N. In Fig. 4-6(b) we show that low temperature ($T<T_c$) spectra normalize to the same

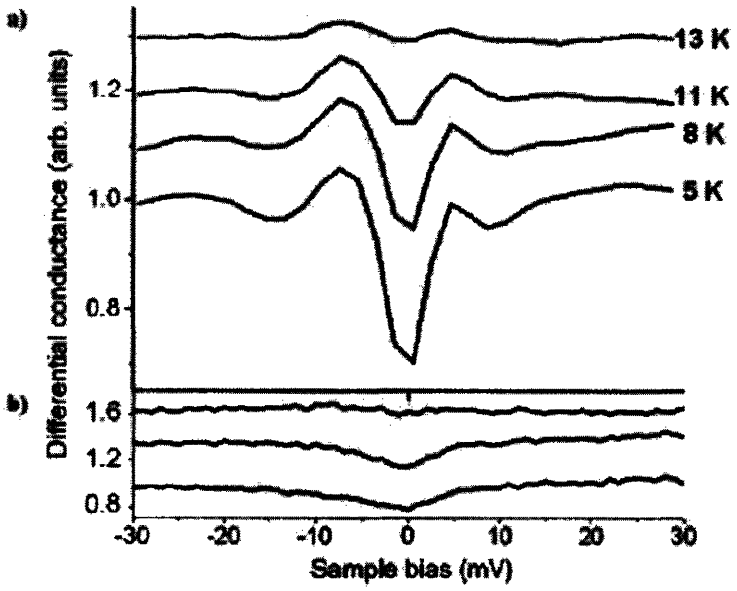

Figure 4-6: (a) Temperature dependence of spatially averaged, normalized spectra at T=5K, 8K, 11K, and 13K. The gap vanishes near T_c=15K. (b) A T=13K spectrum (point A in Fig. 4-1) normalized at T_N=16K (bottom) and T_N=19K (middle) shows insensitivity of our results to the choice of T_N, as both curves show a small gap, in contrast to spectra taken above T_c, which normalize to an ungapped spectrum (top).

small gap regardless of T_N, while high temperature ($T>T_c$) spectra do not. That is, the small gap is present below T_c but not above it. We choose to work with T_N close to T_c because the larger gap is not completely temperature independent and because at higher temperatures thermal broadening begins to obscure the picture.

Chapter 5

Significance of the Two Gaps

We report the first STM imaging of the existence of two gaps in HTSC materials, specifically in overdoped Bi-2201. A natural interpretation of this result is that the gap revealed by normalization, which is homogeneous and vanishes near T_c, is the true superconducting gap and coexists with the large inhomogeneous gap. The large gap is characteristic of a state (likely the pseudogap state) that develops at some temperature above T_c and exists unperturbed down to T=0K (or at least below our measurement temperatures). It is worth noting that even though the samples we are working with are well overdoped, in Bi-2201 the pseudogap phase, which is typically associated with underdoped materials, has been observed to exist in this part of the phase diagram [22, 36, 37]. This coexistence is similar to that observed in the conventional superconductor $NbSe_2$, where a superconducting gap that appears at T_c=7.4K is superimposed on a bowl shaped charge density wave gap that opens at T_{CDW}=35K, and the resulting spectra are the multiplicative product of the two effects [38].

It is reasonable to ask why, after so many years of high resolution STM spectroscopy on a wide variety of high-T_c materials, the superconducting gap may only have been revealed now. One important reason is our newly constructed STM, which is the first capable of making temperature dependent measurements while maintaining a constant position on the sample. This ability is necessary for our normalization technique since previously, all that could have been done was to compare spatially

averaged spectra in temperature. Our STM has allowed us to compare spectra point by point in space in temperature. The large inhomogeneity of the effective background of the pseudogap further highlights the advantage of the ability to normalize spectra point by point. Another reason lies in our choice of sample, Bi-2201, where the energy scales of the small and large gaps are well enough separated that they may both be clearly resolved, whereas most previous STM work had been done on Bi-2212, in which the pseudogap and superconducting gap happen to have similar energy scales [39].

5.1 Comparison with ARPES Results

This result is also consistent with recent angle-resolved photoemission spectroscopy (ARPES) measurements demonstrating the existence of two distinct gaps in both deeply underdoped Bi-2212 [40] and in optimally doped Bi-2201 [41]. ARPES uses the principle of the photoelectric effect by illuminating the sample surface with high energy photons to gather momentum information of the electrons in the sample as a function of the angle at which the photons are scattered off the surface. ARPES probes HTSC in momentum space, and is a nice complimentary technique to STM which probes HTSC in real space. Both of these recent ARPES studies found that in regions of momentum space near the antinode, spectra are characterized by a large gap, while near the node, spectra have a narrow gap. In the case of Bi-2201, Kondo *et al* [41] reported the observation of a small gap with a sharp peak below T_c that closes at T_c in the nodal region of moment space, and a broad gap with a large energy gap of $\sim$40meV that is unchanged across T_c in the antinodal region. Tanaka *et al* [40] found in Bi-2212 the antinodal gap is not characterized by coherence peaks and the gap opening increases with underdoping while the nodal gap has coherence peaks and does not increase with underdoping, suggesting that the two gaps must be of different origins and governed by different mechanisms. Similarly, using Raman spectroscopy on $HgBa_2CuO_{4+x}$, Le Tacon *et al* made the same identification of distinct energy scales found in antinodal and nodal spectra [42].

5.2 Uniting STM Results

Not only is our STM imaging of the two gaps significant in its own light, our results call for an reinterpretation of previous STM results, in the hope of resolving previous controversies introduced by STM measurements for a more unified experimental picture of HTSC.

5.2.1 Smooth Evolution Through T_c

In retrospect, the smooth evolution through T_c observed by STM, first reported by Renner *et al* shown in Fig. 3-4, is most likely the largely temperature-insensitive pseudogap rather than the superconducting gap. The closeness of the energy scales of the two gaps in Bi-2212 near optimal doping is a possible explanation for the interpretation of the pseudogap as the superconducting gap. STM spectral measurement is more sensitive to the antinodal gap because of larger phase space, hence the spectral behavior observed by STM is possibly dominated by the pseudogap rather than the superconducting gap, resulting in the observation of a smooth evolution through T_c.

5.2.2 Nanoscale Inhomogeneity

The nanoscale inhomogeneity reported by STM also deserves to be reevaluated. We have shown that before normalization, the gap maps show large order of inhomogeneity on small scales (Fig. 4-1(b)), similar to what had been reported previously. However, we have shown that this inhomogeneity is due to the broad pseudogap, not the superconducting gap. Moreover, our observations highly suggest that the pseudogap has very little, if anything, to do with high-T_c superconductivity. This interpretation may also explain the low energy homogeneity observed in even very inhomogeneous samples [34, 43, 13], as low energy behavior is dominated by the homogeneous superconducting gap. It also explains why probes of low energy excitations, such as heat capacity measurements [35], as well as STM measurements of

quasi-particle interference patterns [43, 44], are impervious to high energy inhomogeneity.

5.2.3 Subgap Kink

The interpretation of our results also offers a solution to a previously reported mystery in STM spectral measurements—the existence of a ubiquitous subgap kink [34, 8, 13]. Our results suggest that this kink is a manifestation of the small gap that exists on top of the broad pseudogap. Moreover, the ubiquity of this small kink fits well with our observation of the homogeneity of the small gap.

5.3 Uniting Gap Theory

Besides uniting the experimental picture, our findings also represent a unifying step in the two gap picture of HTSC in particular, where a large, spatially inhomogeneous gap (the pseudogap) opens near the antinode above T_c and then coexists with a smaller, spatially homogeneous gap (the superconducting gap) that opens near the node at T_c. The opening of this sharp gap at T_c may prove difficult to explain by "one gap" theories [9, 14, 15, 16, 17, 18, 19], in which the pseudogap and superconducting states differ mostly in the onset of phase coherence, and seems more in line with theories in which the pseudogap is due to some other, possibly competing, phase, in which the magnitude of the pseudogap and superconducting gaps are not directly related [13, 45, 46, 47, 11, 48, 49, 50, 51, 52, 18].

5.4 Future Experimental Directions

Our measurements were done on overdoped Bi-2201. One important future direction is to replicate this study at other dopings and on other materials. In particular, it is important to measure doping dependence in the underdoped regime, where STM and ARPES measured gap widths typically diverge from other measurements [29], and verify that these two gaps follow two different energy scales (superconducting,

T_c, and pseudogap, T*), as indicated by new Raman [42] and ARPES [40] measurements. Even more generally, this normalization technique I have introduced clearly demonstrates the possibility of identifying and disentangling the two gaps of different energy scales. The existence of this technique in itself already lends credit to the co-existing two gap picture, and holds promising potential for further opening up and exploration of this two gap picture in ways that were not available before.

Chapter 6

Conclusion

I have presented the first scanning tunneling microscopic imaging of two gaps in the high temperature superconductor. By using our specially designed temperature variable STM and the new analytical technique of point by point normalization, we observe in a sample of overdoped Pb-$Bi_2Sr_2CuO_{6+\delta}$ of T_c=15K a new, narrow, homogeneous gap that vanishes near T_c, superimposed on the typically observed, inhomogeneous, broad gap, which is only weakly temperature dependent. Not only does this finding strongly support the two gap picture of HTSC, it also suggests that a reinterpretation of previous STM measurements could very well resolve some of the previously reported experimental constroversies between STM and other measurements for a more unified step towards the emergence of a microsopic theory of HTSC.

Appendix A

Data Processing Techniques

All data were organized and processed using the IDL-based package NISTView, originally developed by E.W. Hudson. Several techniques were added in preparing data for the analysis carried out in this thesis. Here I document the most crucial pieces used in this analysis.

A.1 Gap Finder

A gap finding algorithm is used to indentify the gap magnitude Δ from a given spectrum. The algorithm used was orginally written by K. Lang and revised by J. E. Hoffman [5], on top of which I made my own modifications.

Two gap finding algorithms were used. The standard one, "three-of-five" is based on the idea that at the edge of a gap, the slope of the spectrum changes sign. The method begins by identifying the minimum of the spectrum in the middle as the gap center and walking out towards the wings of the spectrum comparing the slope of the spectrum at each data point. The algorithm looks at the slopes of the next five consecutive data points and identifies the first occurance where three out of those five slopes become negative. This is a safeguard measure to reduce false identification of gap due to noise.

The other algorithm introduced is "slope Compare", where again we begin from the minimum of the spectrum in the middle and walk towards the wings of the

spectrum comparing the slope at each data point to the slope at the center of the gap. The gap edge is identified as the first occurance where the slope at the data point falls below a certain fraction of the slope at the center. The need for this algorithm grew out of the observation that most pseudogaps do not have well defined gap edges like coherence peaks in superconducting gaps. There is often just a kink in the spectrum rather than a drastic bending over of the spectrum. Since the slope at the center of the gap is almost always well defined and sharp, looking for the change in the ratio of slopes is a good way to identify these kind of gaps.

A.2 Warping

When the STM is warmed to a new temperature to take a spectral survey over the same region, there is often some thermal drifting of the tip relative to the sample. But to compare and then normalize spectra point by point, it is important to make sure that we match the spectral surveys spatially. To do this, we use the fact that the physical lattice of the sample does not change in temperature, which mean that topographical measurement of the region is constant regardless of temperature. When a spectral survey is taken, a simultaneous topography of the region is also taken. We use this simultaneous topography to match the spectral surveys taken at each temperature.

A survey is taken by making measurements at a grid of locations, which translates into a grid of pixels in the resulting map and corresponding topography image. We use distinct features such as bright atoms in the topography to first roughly correlate the two maps. When the drift is low, we use a linear warping method by visually locating two such markers on each topography, and use their locations in each topography to calculate the stretch factor and the x and y displacements of the second survey relative to the first survey. From this we then calculate a warp which, given the coordinates of a pixel in the first survey, tells us the pixel coordinates in the second survey.

This algorithm is used with the assumption that the drift between the two surveys

is low and linear. We also developed a second algorithm for a more general case, using local correlation to determine the warp pixel by pixel. This is done by first using the linear warping method above to get a rough overall stretch factor and x and y displacements. Then for each pixel in the first topography and its roughly calculated corresponding pixel in the second topography, we take out an equivalent small square area centered on each of the two pixels and perform a correlation map. The position of the maximum correlation tells us the displacement of the pixel in the second survey relative to the pixel in the first survey. The size of the local area used can be decided based on the amount of nonlinear drift present and the pixel resolution of the surveys. Typically, we found that a box-to-image size ratio of 0.3 worked reasonably well. This algorithm is then systematically performed pixel by pixel, creating a warp map that maps the pixels in the second survey to the first survey. For example, warping a topography of size $p_B \times p_B$ (pixels) to a topography of size $p_A \times p_A$ (pixels) would result in a warp map, W, having dimensions $p_A \times p_A \times 2$, where each location $W[i_A, j_A] = (i_B, j_B)$ holds the x and y indices of the corresponding pixel in survey B.

Of course no algorithm in practice is perfect, to reduce error, we implemented a smoothing algorithm that takes the resulting warp map and does a planar fit to the x indices and the y indices respectively. This is based on the expectation that no matter how much drift is present, the survey is taken pixel by pixel in a systematic order, ensuring that neighboring pixels should always be neighboring locations in space.

Using the resulting warp map, we can make a warp-corrected version of the second survey that corresponds point by point to the first survey. To check the quality of the warp, we plot the spectrum at each pixel from the two surveys on top of each other. Even though the spectra feature at high energies vary wildly in space due to inhomogeneity of the broad gap, we see that after warping, the spectra taken at the same location from the two surveys match quite well most of the time in the high energy wings. Since the entire warping process is done solely based on information from topography, we are free to perform independent analysis on the spectroscopy.

Bibliography

[1] H. K. Onnes. *Communications from the Physical Laboratory of the University of Leiden*, 1911.

[2] J. Bardeen, L. N. Cooper, and J. R. Schrieffer. Theory of superconductivity. *Physical Review*, 108:1175–1204, 1957.

[3] J. Orenstein and A. J. Millis. Advances in the physics of high-temperature superconductivity. *Science*, 288:468–74, April 2000.

[4] G. Binnig, H. Rohrer, C. Gerber, and E. Weibel. Surface studies by scanning tunneling microscopy. *Physics Review Letters*, 49:5761, 1982.

[5] J.E. Hoffman. *A Search for Alternative Electronic Order in the High Temperature Superconductor $Bi_2Sr_2CaCu_2O_{8+\delta}$ by Scanning Tunneling Microscopy.* PhD dissertation, UC Berkeley, Department of Physics, 2003.

[6] A. Yazdani, C. M. Howald, C. P. Lutz, A. Kapitulnik, and D. M. Eigler. Impurity-induced bound excitations on the surface of $Bi_2Sr_2CaCu_2O_{8+\delta}$. *Physical Review Letters*, 83:176–179, 1999.

[7] E. W. Hudson, K. M. Lang, V. Madhavan, S. H. Pan, H. Eisaki, S. Uchida, and J. C. Davis. Interplay of magnetism and high-T_c superconductivity at individual Ni impurity atoms in $Bi_2Sr_2CaCu_2O_{8+\delta}$. *Nature*, 411:920–924, 2001.

[8] K. McElroy, Lee Jinho, J. A. Slezak, D. H. Lee, H. Eisaki, S. Uchida, and J. C. Davis. Atomic-scale sources and mechanism of nanoscale electronic disorder in $Bi_2Sr_2CaCu_2O_{8+\delta}$. *Science*, 309:1048–1052, 2005.

[9] P. W. Anderson. The resonating valence bond state in La_2Cuo_4 and superconductivity. *Science*, 235:1196–1198, 1987.

[10] T.R. Chien, Z. Z. Wang, and N. P. Ong. Effect of Zn impurities on the normal-state Hall angle in single-crystal $YBa_2Cu_3O_{6+x}$. *Physical Review Letters*, 67:2088, 1991.

[11] C. M. Varma. Non-Fermi-liquid states and pairing instability of a general model of copper oxide metals. *Physical Review B*, 55:14554–14580, 1997.

[12] J. L. Tallon, G. V. M. Williams, and J. W. Loram. Factors affecting the optimal design of high-T_c superconductors - the pseudogap and critical doping. *Physica C*, 338, 2000.

[13] P. A. Lee, N. Nagaosa, and X.-G. Wen. Doping a Mott insulator: Physics of high-temperature superconductivity. *Review of Modern Physics*, 78:17–85, 2006.

[14] V. B. Geshkenbein, L. B. Ioffe, and A. I. Larkin. Superconductivity in a system with preformed pairs. *Physical Review B*, 55:3173–3180, 1997.

[15] M. Randeria, N. Trivedi, A. Moreo, and R. T. Scalettar. Pairing and spin gap in the normal state of short coherence length superconductors. *Physical Review Letters*, 69:2001–2004, 1992.

[16] V. J. Emery and S. A. Kivelson. Importance of phase fluctuations in superconductors with small superfluid density. *Nature*, 374:434–437, 1995.

[17] M. Franz and A. J. Millis. Phase fluctuations and spectral properties of underdoped cuprates. *Physical Review B*, 58:14572–14580, 1998.

[18] M. Franz and Z. Tesanovic. Algebraic Fermi liquid from phase fluctuations: "topological" Fermions, vortex "Berryons," and QED_3 theory of cuprate superconductors. *Physical Review Letters*, 87:257003, 2001.

[19] P. W. Anderson, P. A. Lee, M. Randeria, T. M. Rice, N. Trivedi, and F. C. Zhang. The physics behind high-temperature superconducting cuprates: the

"plain vanilla" version of RVB. *Journal of Physics Condensed Matter*, 16:755–769, 2004.

[20] C. Renner, B. Revaz, J.-Y. Genoud, K. Kadowaki, and Ø. Fischer. Pseudogap precursor of the superconducting gap in under- and overdoped $Bi_2Sr_2CaCu_2O_{8+\delta}$. *Physical Review Letters*, 80:149–152, 1998.

[21] A. Matsuda, S. Sugita, and T. Watanabe. Temperature and doping dependence of the $Bi_{2.1}Sr_{1.9}CaCu_2O_{8+\delta}$ pseudogap and superconducting gap. *Physical Review B*, 60:1377–1381, 1999.

[22] M. Kugler and Ø. Fischer. Scanning tunneling spectroscopy of $Bi_2Sr_2CuO_{6+\delta}$: New evidence for the common origin of the pseudogap and superconductivity. *Physical Review Letters*, 86(21):4911–4915, 2001.

[23] Ø. Fischer, M. Kugler, I. Maggio-Aprile, and C. Berthod. Scanning tunneling spectroscopy of high-temperature superconductors. *Review of Modern Physics*, 79:353–419, 2007.

[24] Y. Wang, L. Li, and N. P. Ong. Nernst effect in high-T_c superconductors. *Physical Review B*, 73:024510, 2006.

[25] I. Maggio-Aprile, Ch. Renner, A. Erb, E. Walker, and Ø. Fischer. Direct vortex lattice imaging and tunneling spectroscopy of flux lines on $YBa_2Cu_3O_{6+x}$. *Physical Review Letters*, 75:2754, 1995.

[26] S. H. Pan, E. W. Hudson, A. Gupta, K.-W. Ng, H. Eisaki, S. Uchida, and J. C. Davis. STM studies of the electronic structure of vortex cores in $Bi_2Sr_2CaCu_2O_{8+\delta}$. *Physical Review Letters*, 85:1536, 2000.

[27] S.-C. Zhang. A unified theory based on SO(5) symmetry of superconductivity and antiferromagnetism. *Science*, 275:1089, 1997.

[28] S. Chakravarty, R. B. Laughlin, D. K. Morr, and C. Nayak. Hidden order in the cuprates. *Physical Review B*, 63:094503, 2001.

[29] G. Deutscher. Coherence and single-particle excitations in the high-temperature superconductors. *Nature*, 397:410, 1999.

[30] N. Miyakawa, J. F. Zasadzinski, L. Ozyuzer, P. Guptasarma, D. G. Hinks, C. Kendziora, and K. E. Gray. Predominantly superconducting origin of large energy gaps in underdoped $Bi_2Sr_2CaCu_2O_{8+\delta}$ from tunneling spectroscopy. *Physical Review B*, 83:1018–1021, 1999.

[31] R. Cren, D. Roditchev, W. Sacks, and J. Klein. Nanometer scale mapping of the density of states in an inhomogeneous superconductor. *Europhysics Letters*, 54:84–90, 2001.

[32] K. M. Lang, V. Madhavan, J. E. Hoffman, E. W. Hudson, H. Eisaki, S. Uchida, and J. C. Davis. Imaging the granular structure of high-T_c superconductivity in underdoped $Bi_2Sr_2CaCu_2O_{8+\delta}$. *Nature*, 415:412–416, 2002.

[33] S. H. Pan, J. P. O'Neal, R. L. Badzey, C. Chamon, H. Ding, J. R. Engelbrecht, Z. Wang, H. Eisaki, S. Uchida, A. K. Gupta, K. W. Ng, E. W. Hudson, K. M. Lang, and J. C. Davis. Microscopic electronic inhomogeneity in the high-T_c superconductor $Bi_2Sr_2CaCu_2O_{8+\delta}$. *Nature*, 413:282–285, 2001.

[34] C. Howald, P. Fournier, and A. Kapitulnik. Inherent inhomogeneities in tunneling spectra of $Bi_2Sr_2CaCu_2O_{8+\delta}$ crystals in the superconducting state. *Physicsl Review B*, 64:100504, 2001.

[35] J. W. Loram, J. L. Tallon, and W. Y. Liang. Absence of gross static inhomogeneity in cuprate superconductors. *Physical Review B*, 69:060502, 2004.

[36] H. Mashima, N. Fukuo, Y. Matsumoto, G. Kinoda, T. Kondo, H. Ikuta, T. Hitosugi, and T. Hasegawa. Electronic inhomogeneity of heavily overdoped $Bi_{2-x}Pb_xSr_2CuO_y$ studied by low-temperature scanning tunneling microscopy/spectroscopy. *Physical Review B*, 73:060502, 2006.

[37] Guoqing Zheng, P. L. Kuhns, A. P. Reyes, B. Liang, and C. T. Lin. Critical point and the nature of the pseudogap of single-layered copper-oxide. *Physical Review Letters*, 94:047006, 2005.

[38] E. W. Hudson. *Investigating High-T_c Superconductivity on the Atomic Scale by Scanning Tunneling Microscopy.* PhD dissertation, UC Berkeley, Department of Physics, 1999.

[39] H. Ding, T. Yokoya, J. C. Campuzano, T. Takahashi, M. Randeria, M. R. Norman, T. Mochiku, K. Kadowaki, and J. Giapintzakis. Spectroscopic evidence for a pseudogap in the normal state of underdoped high-T_c superconductors. *Nature*, 382:51–54, 1996.

[40] Kiyohisa Tanaka, W. S. Lee, D. H. Lu, A. Fujimori, T. Fujii, Risdiana, I. Terasaki, D. J. Scalapino, T. P. Devereaux, Z. Hussain, and Z. X. Shen. Distinct Fermi-momentum-dependent energy gaps in deeply underdoped Bi2212. *Science*, 314:1910–1913, 2006.

[41] T. Kondo, T. Takeuchi, A. Kaminski, S. Tsuda, and S. Shin. Evidence for two energy scales in the superconducting state of optimally doped $(Bi,Pb)_2(Sr,La)_2CuO_{6+\delta}$. 2006.

[42] M. Le Tacon, A. Sacuto, A. Georges, G. Kotliar, Y. Gallais, D. Colson, and A. Forget. Two energy scales and two distinct quasiparticle dynamics in the superconducting state of underdoped cuprates. *Nature Physics*, 2:537–543, 2006.

[43] K. McElroy, D. H. Lee, J. E. Hoffman, K. M. Lang, J. Lee, E. W. Hudson, H. Eisaki, S. Uchida, and J. C. Davis. Coincidence of checkerboard charge order and antinodal state decoherence in strongly underdoped superconducting $Bi_2Sr_2CaCu_2O_{8+\delta}$. *Physical Review Letters*, 94:197005, 2005.

[44] J. E. Hoffman, K. McElroy, D. H. Lee, K. M. Lang, H. Eisaki, S. Uchida, and J. C. Davis. Imaging quasiparticle interference in $Bi_2Sr_2CaCu_2O_{8+\delta}$. *Science*, 297:1148–1151, 2002.

[45] A. Paramekanti, M. Randeria, and N. Trivedi. Projected wave functions and high temperature superconductivity. *Physical Review Letters*, 87:217002, 2001.

[46] I. Affleck and J. B. Marston. Large-n limit of the Heisenberg-Hubbard model: Implications for high-T_c. *Physical Review B*, 37:3774–3777, 1988.

[47] A. P. Kampf and J. R. Schrieffer. Spectral function and photoemission spectra in antiferromagnetically correlated metals. *Physical Review B*, pages 7967–7974, 1990.

[48] X.-G. Wen and P. A. Lee. Theory of underdoped cuprates. *Physical Review Letters*, 76:503–506, 1996.

[49] S. A. Kivelson, I. P. Bindloss, E. Fradkin, V. Oganesyan, J. M. Tranquada, A. Kapitulnik, and C. Howald. How to detect fluctuating stripes in the high-temperature superconductors. *Review of Modern Physics*, pages 1201–1241, 2003.

[50] J. Zaanen and O. Gunnarsson. Charged magnetic domain lines and the magnetism of high-T_c oxides. *Physical Review B*, 40:7391–7394, 1989.

[51] A. V. Chubukov, D. Pines, and B. P. Stojkovic. Temperature crossovers in cuprates. *Journal of Physics Condensed Matter*, 8:10017–10036, 1996.

[52] M. Vojta and S. Sachdev. Charge order, superconductivity, and a global phase diagram of doped antiferromagnets. *Physical Review Letters*, 83:3916–3919, 1999.